Synthesis, Structures and Electrochemical Properties of Nitro- and Amino-Functionalized Diiron Azadithiolates as Active Site Models of Fe-Only Hydrogenases

Tianbiao Liu,[a] Mei Wang,*[a] Zhan Shi,[b] Hongguang Cui,[a] Weibing Dong,[a] Jiesheng Chen,[b] Björn Åkermark,[c] and Licheng Sun*[a, c]

Abstract: Complex $[\{(\mu\text{-}SCH_2)_2N(4\text{-}NO_2C_6H_4)\}Fe_2(CO)_6]$ (**4**) was prepared by the reaction of the dianionic intermediate $[(\mu\text{-}S)_2Fe_2(CO)_6]^{2-}$ and *N*,*N*-bis(chloromethyl)-4-nitroaniline as a biomimetic model of the active site of Fe-only hydrogenase. The reduction of **4** by Pd-C/H_2 under a neutral condition afforded complex $[\{(\mu\text{-}SCH_2)_2N(4\text{-}NH_2C_6H_4)\}Fe_2(CO)_6]$ (**5**) in 67% yield. Both complexes were characterized by IR, ^1H and ^{13}C NMR spectroscopy and MS spectrometry. The molecular structure of **4**, as determined by X-ray analysis, has a butterfly 2Fe2S core and the aryl group on the bridged-N atom slants to the Fe(2) site. Cyclic voltammograms of **4** and **5** were studied to evaluate their redox properties. It was found that complex **4** catalyzed electrochemical proton reduction in the presence of acetic acid. A plausible mechanism of the electrocatalytic proton reduction is discussed.

Keywords: bioinorganic chemistry · cluster compounds · diiron azadithiolate · iron-only hydrogenase · redox chemistry

Introduction

As molecular hydrogen is a clean and highly efficient fuel, the Fe-only hydrogenase, which is much more efficient in hydrogen production than other types of hydrogenases, has attracted intensive attention in recent years.[1–4] The X-ray crystallographic studies revealed that the active site of Fe-only hydrogenases, so-called H-cluster, contains a 2Fe2S subsite with one of the iron atoms linked to a 4Fe4S cluster by the sulfur atom of a cysteinyl ligand.[5,6] Recently, crystallographic studies and theoretical calculation suggested that the bridging dithiolate ligand feature the bridge of -SCH_2NHCH_2S- (ADT) or the N-protonated equivalent (see below).[7,8]

[a] T. Liu, Prof. M. Wang, H. Cui, W. Dong, Prof. L. Sun
State Key Laboratory of Fine Chemicals
Dalian University of Technology
Zhongshan Road 158–46, Dalian 116012 (China)
Fax: (+86)411-3702185
E-mail: symbueno@vip.sina.com

[b] Z. Shi, Prof. J. Chen
Key Laboratory of Inorganic Synthesis
and Preparative Chemistry
Jilin University, Jiefang Road 119
Changchun 130023 (China)

[c] Prof. B. Åkermark, Prof. L. Sun
Department of Organic Chemistry, Arrhenius Laboratory
Stockholm University, 10691 Stockholm (Sweden)

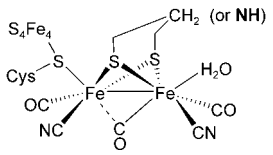

On the basis of the X-ray crystal structures of Fe-only hydrogenases, a variety of 2Fe2S complexes with either a PDT- ($SCH_2CH_2CH_2S$),[9,10] an ADT-[11–13] or a trithiolate-bridge[14,15] were prepared as models of the diiron subsite of H-cluster, and the ligand exchange reactions with all-carbonyl diiron dithiolates were studied intensively.[16–18] Both Darensbourg and Heinekey described H/D exchange reactions of hydride complexes $[(\mu\text{-}H)(\mu\text{-}PDT)Fe(CO)_4(L)_2]$ (L = PMe_3, *t*BuNC).[19–23] Rauchfuss and co-workers reported the electrochemical reduction of protons to H_2 catalyzed by PDT-bridged diiron complexes in the presence of a strong proton acid, H_2SO_4, HCl or HOTs,[24–26] whereas Darensbourg and co-workers reported that 2Fe2S model complexes can act as catalysts for electrochemical H_2 evolution in the presence of a weak proton acid (HOAc).[27] The functional and structural mimics of the diiron subsite of Fe-only hydrogenases can shed light on the working mechanism of their active site and enable us to eventually produce molecular hydrogen using biomimetic catalyst systems.

We are interested in the concept of light-driven proton reduction by an artificial supramolecular system,[28–31] which is

  DOI: 10.1002/chem.200400004

composed of a biomimetic model of the hydrogenase active site and a light-harvesting component. In order to attach a 2Fe2S subsite model to a photosensitive species, a suitable functional group should be introduced on the azadithiolate bridge. Here we report the preparation and electrochemical properties of nitro- and amino-functionalized diiron azadithiolates, $[\{(\mu\text{-}SCH_2)_2N(4\text{-}NO_2C_6H_4)\}Fe_2(CO)_6]$ (**4**) and $[\{(\mu\text{-}SCH_2)_2N(4\text{-}NH_2C_6H_4)\}Fe_2(CO)_6]$ (**5**), as well as the molecular structure of **4**. Complex **5** with an amino-functionalized bridging-azadithiolate ligand is ready to be linked to a redox active species for the further studies of electron-transfer processes and redox level changes of the novel supramolecular system.

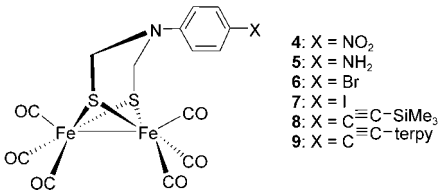

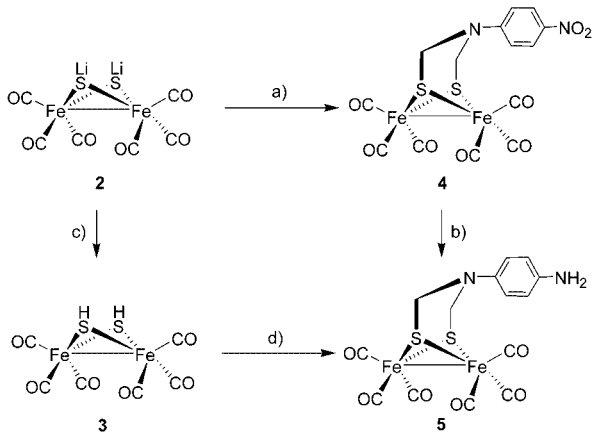

Scheme 1. a) $(ClCH_2)_2N(4\text{-}NO_2C_6H_4)$ (**1**), THF, −78 °C, 2 h; b) Pd/C, H_2, CH_3OH, 30 °C, 18 h; c) F_3CCOOH, THF, −78 °C, 20 min; d) *p*-$C_6H_4(NH_2)_2$, paraformaldehyde, THF, 4 h.

Results and Discussion

Synthesis and spectroscopic characterization of complexes 4 and 5: Very recently, we have reported an amino-functionalized model of the diiron subsite prepared by the reaction of 1,3-propanedithiol and $[Fe_3(CO)_{12}]$.[29] Early in our work, we tried to synthesize the nitro-functionalized diiron azadithiolate by the reaction of $[Fe_3(CO)_{12}]$ and *N*-(4-nitrophenyl)-2-aza-1,3-propanedithiol, but did not get the desired product. The synthetic route was thus adapted to Rauchfuss' protocol (Scheme 1).[11] Treatment of lithium salt (**2**), freshly derived from $[(\mu\text{-}S)_2Fe_2(CO)_6]$ (**3**), with *N*,*N*-bis(chloromethyl)-4-nitroaniline (**1**) gave complex **4** in a good yield. Different methods were explored to reduce complex **4** to an amino-functionalized complex **5**. The reduction of the NO_2 group of complex **4** by Sn/HCl gave complex **5** in a very low yield. Characterization of the reduced products of complex **4** showed that the frame structure of **4** decomposed in a hot acidic aqueous solution. The attempt to reduce compound **1** to *N*,*N*-bis(chloromethyl)-4-aminoaniline prior to the combination with the diiron part was unsuccessful because compound **1** is not thermostable above 0 °C. However, complex **5** was obtained in a reasonable yield by the reduction of complex **4** using Pd/C/H_2 under mild and neutral conditions. Complex **5** could also be obtained in 20% yield via a straightforward reaction of $[(\mu\text{-}SH)_2Fe_2(CO)_6]$ with a premixed THF solution of paraformaldehyde and *p*-phenylenediamine (Scheme 1). Complexes **4** and **5** were stable to air in the solid state but moderately sensitive in solution.

Complexes **4** and **5** were characterized by IR, ^1H and ^{13}C NMR spectroscopy and MS spectrometry. The mass spectra of API-ES positive mode show the parent ion peaks at *m*/*z* 531 $[M+Na]^+$ for **4** and 479 $[M+H]^+$ for **5**. The IR spectra of complexes **4** and **5** in CH_2Cl_2 each show three strong CO bands in the region of 1990–2080 cm^{-1}. Two characteristic NO_2 frequencies at 1520 and 1325 cm^{-1} for **4** and a weak NH_2 band at 3370 cm^{-1} for **5** were observed. Table 1 shows a comparison of CO bands for **4**, **5** and some related diiron aryl-azadithiolates $[\{(\mu\text{-}SCH_2)_2N(4\text{-}XC_6H_4)\}Fe_2(CO)_6]$ (X = Br (**6**), I (**7**), trimethylsilylethynyl (**8**), and [4′-(2,2′:6′, 2″-terpyridyl)]ethynyl (**9**)).[28,32] The values of CO bands of complex **4** are quite similar to those reported for its analogues **6**–**9**, while the CO bands of amino-functionalized **5** move by 4–6 cm^{-1} to lower wavenumbers, implicating that the electron releasing effect of the NH_2 group on the *para*-position of the benzene ring does have a subtle impact on the electronic property of the carbonyl ligands.

Table 1. A comparison of CO bands of analogous diiron aryl-azadithiolate complexes $[\{(\mu\text{-}SCH_2)_2N(4\text{-}XC_6H_4)\}Fe_2(CO)_6]$.

Complex	X	CO bands (CH_2Cl_2, cm^{-1})	Ref.
4	NO_2	2077 m, 2040 s, 2003vs	this work
5	NH_2	2073 m, 2034 s, 1998vs	this work
6	Br	2077 m, 2038 s, 2000vs	[32]
7	I	2076 m, 2038 s, 2000vs	[32]
8	C≡C-$SiMe_3$	2076 m, 2038 s, 2001vs	[32]
9	C≡C-terpy	2076 m, 2038 s, 2001vs	[28]

Compared with the signals of **4**, the corresponding signals of **5** are upfield-shifted owing to different electronic effects of NO_2 and NH_2 groups. The hydrogen atoms of the benzene ring present themselves as two singlets for **4** and a broad singlet for **5**, assuming that the reduction of the NO_2 group makes the chemical environments for the four hydrogen atoms of the benzene ring alike. In the ^{13}C NMR spectra, the signals of the carbon atoms of **5** are also shifted upfield compared with the corresponding ones of **4**. The similar chemical environment for two *ipso*-C atoms, each of which is attached to an amino-N atom of the benzene ring in complex **5**, lead to analogous chemical shifts ($\delta = 140.40$ and 138.21).

Molecular structure of 4: The crystallographic structure of **4** is given as an ORTEP diagram in Figure 1. Selected bond

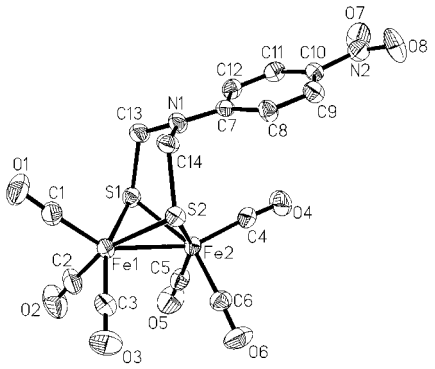

Figure 1. ORTEP (ellipsoids at 30% probability) diagram of **4**.

lengths and bond angles are listed in Table 2. Crystallographic study of **4** shows the structural resemblance of **4** with the active site of Fe-only hydrogenases.[5,6] As previous-

Table 2. Selected bond lengths [Å] and angles [°] for complex **4**.

Fe(1)–Fe(2)	2.4998(10)	Fe(1)-S(1)-Fe(2)	66.98(4)
Fe(1)–S(1)	2.724 (13)	Fe(1)-S(2)-Fe(2)	67.06(4)
Fe(1)–S(2)	2.2561(12)	S(1)-Fe(1)-S(2)	85.36(4)
Fe(2)–S(1)	2.2576(13)	S(1)-Fe(2)-S(2)	85.40(5)
Fe(2)–S(2)	2.2694(10)	C(13)-S(1)-Fe(1)	111.32(12)
Fe(1)–C(1)	1.798(4)	C(14)-S(2)-Fe(1)	106.56(12)
Fe(1)–C(2)	1.8805(4)	C(1)-Fe(1)-C(2)	99.85(18)
Fe(1)–C(3)	1.790(4)	C(2)-Fe(1)-C(3)	92.32(19)
N(1)–C(7)	1.388(4)	C(3)-Fe(1)-C(1)	97.23(17)
N(1)–C(14)	1.432(4)	C(1)-Fe(1)-S(2)	100.89(12)
N(1)–C(13)	1.423(4)	C(1)-Fe(1)-S(1)	103.84(12)
S···S	3.070	C(7)-N(1)-C(13)	123.5(3)
		C(7)-N(1)-C(14)	121.2(3)
		C(13)-N(1)-C(14)	113.0(3)

ly reported 2Fe2S models, the central 2Fe2S structure is in a butterfly conformation and each Fe atom is coordinated with a pseudo-square-pyramidal geometry. The Fe–Fe distance (2.4998 Å) is somewhat shorter than that in the structures of DdHase and CpHase (ca. 2.6 Å)[5–7] and in good agreement with the structural data of Fe–Fe bonds (2.49–2.51 Å) found in other diiron azadithiolates.[12,13,28] The bridged-N atom is not in the plane defined by the C(7), C(13), and C(14) atoms. The sum of the C-N-C angles around N is 357.7°. The slight distortion of the planar shape of the sp^2-hybridized N(1) atom can somewhat weaken the p-π conjugation between the phenyl ring and the p orbital of the bridged-N atom, resembling the situation in other two structural examples of diiron aryl-azadithiolates reported very recently.[28] The structural character may greatly influence electron-transfer processes in the designed molecular assembly of model complex **5** and a photosensitive species. The 4-nitrophenyl group slants towards the Fe(2) site, and the axial through N(1), C(7), C(10) and N(2) atoms is approximately parallel to the apical carbonyl ligand (C(4)-O(4)) on the Fe(2) atom. The Fe(2)$(CO)_3$ unit that lies under the nitroaryl ring is perturbed by the long range interaction. The angle of C(4)-Fe(2)-Fe(1) (155.06(10)°) is enlarged by 6.9° compared with that of C(1)-Fe(1)-Fe(2) (148.20(12)°). The latter is quite similar with the corresponding angles (148.31(9)°) for the PDT-bridged analogue $[(\mu\text{-PDT})Fe_2(CO)_6]$,[10] in which two Fe$(CO)_3$ moieties are symmetric. The preliminary studies on the ligand-exchange reactions showed that one of the CO ligands on the Fe(1) atom could be substituted by PPh_3, but due to the spatial requirements of the 4-nitrophenyl group, the further displacement of the CO ligands on the Fe(2) atom was thwarted. Another evidence for the CO-monosubstitution to Fe(1) by PPh_3 is the formation of an analogous complex $[\{(\mu\text{-}SCH_2)_2N(4\text{-}BrC_6H_4)\}Fe_2(CO)_5(PPh_3)]$, the structural study of which shows that the PPh_3 ligand is coordinated to Fe(1) in the apical position.[32]

Electrochemistry of model complexes 4 and 5: Cyclic voltammograms of model complexes **4** and **5** (Figure 2) were studied to evaluate their redox properties since the iron core plays a key role in the formation of Fe-H hydride and the process of H_2 evolution by Fe-only hydrogenases. Electrochemical data of PDT- and EDT-bridged (SCH_2CH_2S) diiron complexes as well as diiron dialkylthioates have been reported in the literature of recent years,[24–27,33,34] but very few data on ADT-bridged diiron model complexes have been reported.[32] The cyclic voltammograms for **4** and **5** were recorded in CH_3CN (with 0.05 M nBu_4NPF_6 as electrolyte) and the electrochemical data were given in Table 3. An irreversible oxidation and two quasi-reversible reduction peaks were observed for **4** (labeled by 1, 2 and 3 in Figure 2a), while complex **5** manifested an irreversible reduc-

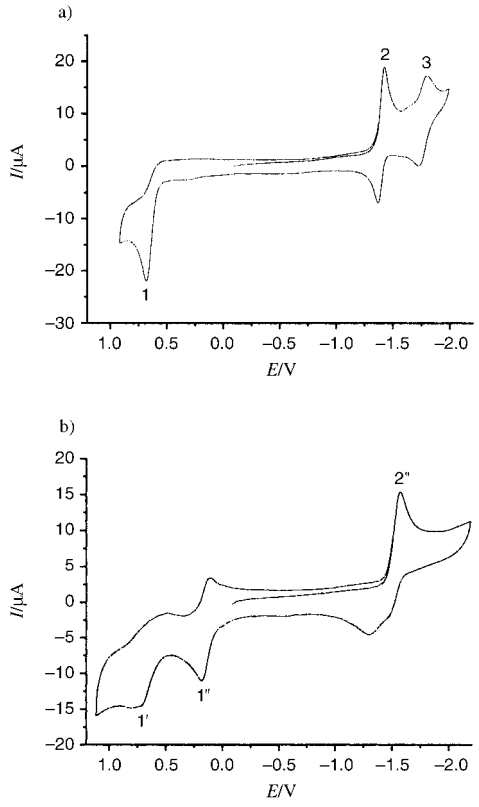

Figure 2. Cyclic voltammograms of **4** (a) and **5** (b), 1.0 mmol in 0.05 M nBu_4NPF_6/CH_3CN at a scan rate of 100 mV s^{-1}.

Table 3. Electrochemical data of complexes **4** and **5**.[a]

Compound	E_{pirr}^{ox} [V] Fe^IFe^I/ $Fe^{II}Fe^I$	E_{pa}, E_{pc} [V] Oxidation of NH_2	E_{pc}, E_{pa} [V] Fe^IFe^I/ Fe^0Fe^I	E_{pc}, E_{pa} [V] Fe^0Fe^I/ Fe^0Fe^0
4	+0.78	–	−1.34, −1.28	−1.71, −1.63
5	+0.80	+0.28, +0.20	−1.48, −1.23	–
[(μ-PDT)$Fe_2(CO)_6$]	+0.84	–	−1.57, −1.47	E_{pc} = −2.11

[a] All potentials in Table 3 are versus Ag/Ag^+ (0.01 M $AgNO_3$ in CH_3CN).

tion peak together with an irreversible and a quasi-reversible oxidation peaks (labeled by 2′, 1′ and 1″ in Figure 2b). The irreversible oxidation peaks (labeled by 1 and 1′) at +0.78 V vs. $Ag/AgNO_3$ for **4** and +0.80 V for **5** are ascribed to the $[Fe^IFe^I]\rightarrow[Fe^{II}Fe^I]+e^-$ process as described for the PDT-bridged diiron complex [(μ-PDT)$Fe_2(CO)_6$] by Darensbourg and co-workers.[27] The extra quasi-reversible oxidation peak at +0.28 V for **5** (peak 1″ in Figure 2b), which is not observed in the cyclic voltammogram of **4**, is presumably assigned to the oxidation of the NH_2 group of **5**. By comparison with the electrochemical studies of [(μ-PDT)$Fe_2(CO)_6$], [(μ-$SR)_2Fe_2(CO)_6$] and their derivatives,[24–27] the reduction peaks at −1.34 V for **4** and −1.48 V for **5** are assigned to a one-electron process $[Fe^IFe^I]+e^-\rightarrow[Fe^0Fe^I]$ (E_1) and the peak at −1.71 V for **4** to the second electron-transfer process $[Fe^0Fe^I] + e^-\rightarrow[Fe^0Fe^0]$ (E_2). The second reduction peak of **5** is not accessible within the solvent window in Figure 2b. The first reduction peak of **5** shifts to a more negative potential by 140 mV (peak 2′ in Figure 2b) compared with the corresponding one of **4** (peak 2 in Figure 2a). A comparison of the reduction potentials of **4** and **5** shows that complex **4** is more readily reduced, suggesting that the different electronic effects of the NO_2 and NH_2 groups of the benzene ring result in somewhat different electron density at the iron core of **4** and **5**. This is also shown by the reduction potential (cathodic peak potential, −1.44 V vs. $Ag/AgNO_3$) of the corresponding bromo-substituted complex **6**.[32] Interestingly the reduction potentials of **4** and **5** are less negative than that for the PDT-bridged all-carbonyl diiron complex (see Table 3), which indicates that ADT-bridged model complexes are in general more easily reduced than the PDT-bridged analogues.

The behavior of catalytic proton reduction by **4** was studied by cyclic voltammograms in the presence of a weak acid, HOAc (0–10 mmol) in CH_3CN (Figure 3). The current intensity of the first reduction peak at −1.34 V for **4** apparently increased with an anodic shift by 60 mV as 2 mmol of HOAc was added, and the current intensity of it did not grow up further with sequential increments of the acid concentration. A sharp increase in the current height of the initial second reduction peak at −1.71 V for **4** with an obvious anodic shift by 230 mV was observed as 2 mmol of HOAc was added. The height of the second reduction peak of **4** continuously grew with increased acid concentration, which is a characteristic of an electrochemical catalytic process. The quasi-reversibility of both reduction peaks of **4** disappeared upon the addition of HOAc. A noteworthy point in the cyclic voltammograms of **4** with variable amount of HOAc is that the reduction peaks obviously move to more positive potentials in the presence of 2 equiv HOAc. In contrast, the carbon chain-bridged all-carbonyl diiron complexes did not show any anodic shift of the reduction potentials in the presence of a proton acid.[24–27] The distinctly different electrochemical behavior of the ADT-bridged diiron complex **4** from carbon chain-bridged all-carbonyl diiron complexes is undoubtedly caused by the introduction of the nitrogen atom to the bridge, which can be protonated in the presence of a proton acid. The cyclic voltammograms of **4** suggest a CECE (chemical-electrochemical-chemical-electrochemical) mechanism for the electrochemical catalysis of proton reduction by the ADT-bridged all-carbonyl Fe^IFe^I model complex **4** (Scheme 2), which is different from the

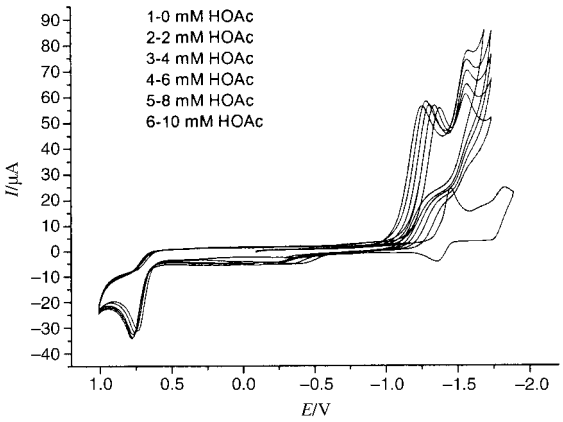

Figure 3. Cyclic voltammogram of **4** (1.0 mmol) with HOAc (0–10 mmol).

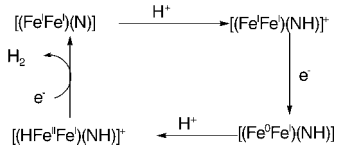

Scheme 2. A plausible CECE mechanism for electrocatalytic proton reduction by **4** in the presence of HOAc.

EECC (electrochemical-electrochemical-chemical-chemical) process supposed for the carbon chain-bridged all-carbonyl Fe^IFe^I models.[27] In the presence of HOAc, complex **4** is instantly protonated on the bridged-N atom to form $[(Fe^IFe^I)(NH)]^+$ ($\mathbf{4H}^+$), resulting in an anodic shift of the reduction potential. The $[(Fe^0Fe^I)(NH)]$ species, consequently derived from electrochemical reduction of $[\mathbf{4H}]^+$, is further protonated on the electron-enriched iron core to generate an $[(HFe^{II}Fe^I)(NH)]^+$ intermediate, which can evolve H_2 with a second one-electron reduction of $[(Fe^{II}Fe^I)(N)]^+$ to $[(Fe^IFe^I)(N)]$ species to fulfill the catalytic cycle.

Conclusion

Nitro- and amino-functionalized diiron azadithiolate complexes [{(μ-$SCH_2)_2N(4\text{-}NO_2C_6H_4)$}$Fe_2(CO)_6$] (**4**) and [{(μ-

$SCH_2)_2N(4\text{-}NH_2C_6H_4)\}Fe_2(CO)_6]$ (**5**) were synthesized as biomimetic models of the diiron subsite of H-cluster. The NO_2 group of **4** can be effectively reduced to the NH_2 group by Pd-C/H_2 under mild conditions without affecting the framework of **4**, while it was decomposed on reduction by Sn/HCl in a hot acidic aqueous solution. Spectroscopic and electrochemical analyses of **4** and **5** indicate that the substituent of an aromatic ring on the bridging-N atom does have an observable influence on the electronic properties of the iron core and carbonyl ligands. A CECE mechanism is tentatively proposed for the electrochemical catalysis of proton reduction in the presence of HOAc. This is based on the cyclic voltammograms of **4** and is in contrast to the EECC process suggested for carbon chain-bridged all-carbonyl Fe^IFe^I model complexes. It gives a hint that introduction of a nitrogen atom to the bridge may change the electrocatalytic processes of diiron models. In order to investigate electron-transfer and proton-reduction processes, we are trying to construct supramolecular systems by connecting the amino group of **5** with various redox active species.

Experimental Section

Reagents and instruments: All reactions and operations related to organometallic complexes were carried out under a dry, oxygen-free dinitrogen atmosphere with standard Schlenk techniques. All solvents were dried and distilled prior to use according to the standard methods. Commercially available chemicals, paraformaldehyde, 4-nitroaniline, *p*-$C_6H_4(NH_2)_2$ and $[Fe(CO)_5]$ were used without further purification. The reagent $LiEt_3BH$ was purchased from Aldrich. Starting compounds *N*,*N*-bis(chloromethyl)-4-nitroaniline (**1**), $[(\mu\text{-}S)_2Fe_2(CO)_6]$ and $[(\mu\text{-}LiS)_2Fe_2(CO)_6]$ (**2**) were prepared according to the literature procedures.[11,35,36] Lithium salt **2** was used in situ immediately for the further reaction.

IR spectra were recorded on a JASCO FT/IR 430 spectrophotometer. Proton and ^{13}C NMR spectra were collected on a Varian INOVA 400NMR spectrometer. Mass spectra were recorded on an HP1100 MSD instrument. Elemental analyses were performed on a CARLO ERBA MOD-1106 elemental analyzer.

Synthesis of $[\{(\mu\text{-}SCH_2)_2N(4\text{-}NO_2C_6H_4)\}Fe_2(CO)_6]$ (4): A solution of 4-$NO_2C_6H_4N(CH_2Cl)_2$ (1.00 g, 4.3 mmol) in THF (5 mL) was added to a THF solution (20 mL) of **2** at −78 °C, freshly derived from $[(\mu\text{-}S)_2Fe_2(CO)_6]$ (1.00 g, 2.9 mmol) and $LiEt_3BH$ (1 M in THF, 6.0 mL, 6.0 mmol). The mixture was stirred for 2 h at −78 °C and the solution turned dark red from dark emerald green. After filtration, solvent was removed from the filtrate on a rotary evaporator. The crude product was purified by column chromatography with silica gel by using CH_2Cl_2/Et_3N (100:0.3) as eluent to give complex **4** as a dark red solid (1.35 g, 91 %). Recrystallization in CH_2Cl_2/pentane afforded crystals of **4** suitable for X-ray crystallography study. ^1H NMR ($CDCl_3$): $\delta = 8.22$ (d, 2H), 7.26 (d, 2H), 4.33 (s, 4H); ^{13}C NMR ($CDCl_3$): $\delta = 206.53$, 149.32, 140.10, 126.39, 114.28, 49.36; IR (CH_2Cl_2): $\tilde{\nu} = 2077$ (m), 2040 (s)/2003 (vs) (CO), 1520 (m)/1325 cm^{-1} (m) (NO_2); MS (API-ES): *m*/*z*: 531 $[M+Na^+]$; elemental analysis calcd (%) for $C_{14}H_8N_2O_8S_2Fe_2$ (508.04): C 33.10, H 1.59, N 5.51; found: C 32.97, H 1.61, N 5.48.

Synthesis of $[\{(\mu\text{-}SCH_2)_2N(4\text{-}NH_2C_6H_4)\}Fe_2(CO)_6]$ (5)

Method A: A methanol solution (40 mL) of complex **4** (200 mg, 0.39 mmol) and the catalyst Pd/C powder (10 %, 180 mg) was added to a 75 mL stainless steel autoclave equipped with a magnetic bar. The autoclave was charged with 0.4 MPa of H_2. After the mixture was stirred at 30 °C for 6 h, the hydrogen pressure of the autoclave went down to 0.2 MPa and the autoclave was recharged to 0.4 MPa. After stirred for 18 h, the solution was dried with anhydrous Na_2SO_4 (5 g), then filtered and concentrated in vacuo to give a dark purple solid, which was purified by column chromatography with silica gel using CH_2Cl_2 as eluent. Complex **5** was obtained in a yield of 67 % (0.13 g). ^1H NMR ($CDCl_3$): $\delta =$ 6.63 (br s, 4H), 4.20 (s, 4H), 3.42 (s, 2H); ^{13}C NMR ($CDCl_3$): $\delta = 207.22$, 140.40, 138.21, 118.45, 116.77, 50.94; IR (CH_2Cl_2): $\tilde{\nu} = 2073$ (m), 2034 (s)/1998 (vs) (CO), 3372 cm^{-1} (w) (NH_2); MS (API-ES): *m*/*z*: 479 $[M+H]^+$; elemental analysis calcd (%) for $C_{14}H_{10}N_2O_6S_2Fe_2$ (478.06): C 35.17, H 2.11, N 5.86; found: C 35.53, H 2.05, N 5.67.

Method B: A mixture of paraformaldehyde (0.6 g, 20 mmol) and *p*-phenylenediamine (1.08 g, 10 mmol) in THF (20 mL) was stirred for 6 h. A solution of $[(\mu\text{-}SH)_2Fe_2(CO)_6]$ (0.2 g, 0.57 mmol) in THF (20 mL) was then added to the above suspension. After stirred for 8 h, a dark solution was obtained and filtrated. Solvent was removed from the filtrate in vacuo to afford a dark purple solid. The crude product was purified by column chromatography with CH_2Cl_2 as eluent to give complex **5** as a purple crystalline solid (54 mg, 20 %).

X-ray crystal structure determination of 4: A dark red crystal with approximate dimensions of 0.40 × 0.30 × 0.30 mm was mounted in air. Diffraction measurements were made on a Siemens SMART CCD diffractometer using graphite monochromated $Mo_{K\alpha}$ radiation ($\lambda = 0.71073$ Å). Complete crystal data and parameters for data collection and refinement are listed in Table 4. Data processing was accomplished with the SAINT processing program.[37] Intensity data were corrected for absorption with empirical methods. The structure was solved by direct methods and refined by full-matrix least-squares techniques on F_o^2 by using the SHELXTL crystallographic software package.[38] All hydrogen atoms were located by difference maps and their positions were refined isotropically. All non-hydrogen atoms were refined anisotropically.

Table 4. X-ray Crystallographic data for **4**.

formula	$C_{14}H_8N_2O_8{\cdot}Fe_2S_2$
M_w	508.04
crystal system	triclinic
space group	$P\bar{1}$
a [Å]	7.935(2)
b [Å]	10.646(3)
c [Å]	12.142(6)
α [°]	109.771(18)
β [°]	100.70(3)
γ [°]	91.87(2)
V [Å^3]	943.4(6)
Z	2
ρ_{calcd} [g m^{-3}]	1.789
T [K]	298
μ [mm^{-1}]	1.804
F [000]	508
reflns measured	2567
reflns observed [$I > 2\sigma(I)$]	2559
parameters	253
GOF (on F^2)	1.011
*R*1 [$I > 2\sigma(I)$]	0.0304[a]
*wR*2 [$I > 2\sigma(I)$]	0.0792[b]
residual electron density [e Å^{-3}]	0.345, −0.321

[a] $R1 = (\Sigma||F_o|-|F_c||)/(\Sigma|F_o|)$. [b] $wR2 = [\Sigma w(F_o^2-F_c^2)^2/\Sigma w(F_o^2)^2]^{1/2}$.

CCDC-215491 (**4**) contains the supplementary crystallographic data for this paper. These data can be obtained free of charge via www.ccdc.cam.ac.uk/conts/retrieving.html (or from the Cambridge Crystallographic Data Centre, 12 Union Road, Cambridge CB2 1EZ, UK; fax: (+44)1223-336-033; or e-mail: deposit@ccdc.cam.ac.uk).

Electrochemistry: Acetonitrile (Aldrich, spectroscopy grade) used for performance of electrochemistry was dried with molecular sieve (4) Å) and then freshly distilled from CaH_2 under N_2. A solution of 0.05 M nBu_4NPF_6 (Fluka, electrochemical grade) in CH_3CN was used as electrolyte. Electrochemical measurements were recorded using a BAS-100W electrochemical potentiostat. The electrolyte solution was degassed by bubbling with dry argon for 10 min before measurement. Cyclic voltammograms were obtained in a three-electrode cell under argon. The working electrode was a glassy carbon disc (diameter 3 mm) successively polished with 3 and 1 μm diamond pastes and sonicated in ion-free water for

10 min. The reference electrode was a non-aqueous Ag/Ag^+ electrode (0.01 M $AgNO_3$ in CH_3CN) and the auxiliary electrode was a platinum wire.

Acknowledgement

We are grateful to the Ministry of Science and Technology of China and the Chinese National Natural Science Foundation (Grant no. 20128005 and 20173006) for financial supports of this work.

[1] R. Cammack, *Nature* **1999**, *397*, 214–215.
[2] D. J. Evans, C. J. Pickett, *Chem. Soc. Rev.* **2003**, *32*, 268–275.
[3] M. Y. Darensbourg, E. J. Lyon, J. J. Smee, *Coord. Chem. Rev.* **2000**, *206–207*, 533–561.
[4] M. Frey, *ChemBioChem* **2002**, *3*, 153–160.
[5] J. W. Peters, W. N. Lanzilotta, B. J. Lemon, L. C. Seefeldt, *Science* **1998**, *282*, 1853–1858.
[6] Y. Nicolet, C. Piras, P. Legrand, C. E. Hatchikian, J. C. Fontecilla-Camps, *Structure* **1999**, *7*, 13–23.
[7] Y. Nicolet, A. L. Lacey, X. Vernéde, V. M. Fernandez, E. C. Hatchikian, J. C. Fontecilla-Camps, *J. Am. Chem. Soc.* **2001**, *123*, 1596–1601.
[8] H. J. Fan, M. B. Hall, *J. Am. Chem. Soc.* **2001**, *123*, 3828–3829.
[9] M. Schmidt, S. M. Contakes, T. B. Rauchfuss, *J. Am. Chem. Soc.* **1999**, *121*, 9736–9737.
[10] E. J. Lyon, I. P. Georgakaki, J. H. Reibenspies, M. Y. Darensbourg, *Angew. Chem.* **1999**, *111*, 3373; *Angew. Chem. In. Ed.* **1999**, *38*, 3178–3180.
[11] J. D. Lawrence, H. Li, T. B. Rauchfuss, *Chem. Commun.* **2001**, 1482–1483.
[12] J. D. Lawrence, H. Li, T. B. Rauchfuss, M. Bénard, M. Rohmer, *Angew. Chem.* **2001**, *113*, 1818; *Angew. Chem. Int. Ed.* **2001**, *40*, 1768–1771.
[13] H. Li, T. B. Rauchfuss, *J. Am. Chem. Soc.* **2002**, *124*, 726–727.
[14] S. J. George, Z. Cui, M. Razavet, C. J. Pickett, *Chem. Eur. J.* **2002**, *8*, 4037–4046.
[15] W. Liaw, W. Tsai, H. Gau, C. Lee, S. Chou, W. Chen, G. Lee, *Inorg. Chem.* **2003**, *42*, 2783–2788.
[16] A. L. Cloiree, S. P. Best, S. Borg, S. C. Davies, D. J. Evans, D. L. Hughes, C. J. Pickett, *Chem. Commun.* **1999**, 2285–2286.
[17] E. J. Lyon, I. P. Georgakaki, J. H. Reibenspies, M. Y. Darensbourg, *J. Am. Chem. Soc.* **2001**, *123*, 3268–3278.
[18] J. D. Lawrence, T. B. Rauchfuss, S. R. Wilson, *Inorg. Chem.* **2002**, *41*, 6193–6195.
[19] X. Zhao, I. P. Georgakaki, M. L. Miller, J. C. Yarbrough, M. Y. Darensbourg, *J. Am. Chem. Soc.* **2001**, *123*, 9710–9711.
[20] X. Zhao, I. P. Georgakaki, M. L. Miller, R. Mejia-Rodriguez, C. Chiang, M. Y. Darensbourg, *Inorg. Chem.* **2002**, *41*, 3917–3928.
[21] I. P. Georgakaki, M. L. Miller, M. Y. Darensbourg, *Inorg. Chem.* **2003**, *42*, 2489–2494.
[22] X. Zhao, C. Chiang, M. L. Miller, M. V. Rampersad, M. Y. Darensbourg, *J. Am. Chem. Soc.* **2003**, *125*, 518–524.
[23] J. L. Nehring, D. M. Heinekey, *Inorg. Chem.* **2003**, *42*, 4288–4292.
[24] F. Gloaguen, J. D. Lawrence, T. B. Rauchfuss, *J. Am. Chem. Soc.* **2001**, *123*, 9476–9477.
[25] F. Gloaguen, J. D. Lawrence, M. Schmidt, S. R. Wilson, T. B. Rauchfuss, *J. Am. Chem. Soc.* **2001**, *123*, 12518–12527.
[26] F. Gloaguen, J. D. Lawrence, T. B. Rauchfuss, M. Bénard, M. Rohmer, *Inorg. Chem.* **2002**, *41*, 6573–6582.
[27] D. Chong, I. P. Georgakaki, R. Mejia-Rodriguez, J. Sanabria-Chinchilla, M. P. Soriaga, M. Y. Darensbourg, *J. Chem. Soc. Dalton Trans.* **2003**, 4158–4163.
[28] S. Ott, M. kritikos, B. Åkermark, L. Sun, *Angew. Chem.* **2003**, *115*, 3407; *Angew. Chem. Int. Ed.* **2003**, *42*, 3285–3288.
[29] S. Salyi, M. Kritikos, B. Åkermark, L. Sun, *Chem. Eur. J.* **2003**, *9*, 557–560.
[30] H. Wolpher, M. Borgström, L. Hammarström, J. Bergquist, V. Sundström, S. Styring, L. Sun, B. Åkermark, *Inorg. Chem. Commun.* **2003**, *6*, 989–991.
[31] Y. Amao, I. Okura, *J. Mol. Catal. B* **2002**, *17*, 9–21.
[32] S. Ott, M. Kritikos, B. Åkermark, L. Sun, R. Lomoth, *Angew. Chem.* **2004**, *116*, 1024–1027; *Angew. Chem. Int Ed.* **2004**, *43*, 1006–1009.
[33] W. Liaw, N. Lee, C. Chen, C. Lee, G. Lee, S. Peng, *J. Am. Chem. Soc.* **2000**, *122*, 488–494.
[34] M. Razavet, S. C. Davies, D. L. Hughes, J. E. Barclay, D. J. Evans, S. A. Fairhurst, X. Liu, C. J. Pickett, *J. Chem. Soc. Dalton Trans.* **2003**, 586–595.
[35] D. Seyferth, R. S. Henderson, L. Song, *Organometallics* **1982**, *1*, 125–133.
[36] D. Seyferth, R. S. Henderson, *J. Organomet. Chem.* **1981**, *218*, C34–C36.
[37] Software packages SMRT and SAINT, Siemens Analytical X-Ray Instruments Inc., Madison, WI, **1996**.
[38] SHELXTL, Version 5.1, Siemens Industrial Automation, Inc. **1997**.

Received: January 4, 2004
Published online: July 28, 2004

